Int J Adv Manuf Technol (2015) 78:1053–1065
DOI 10.1007/s00170-014-6700-z

ORIGINAL ARTICLE

Multi-objective optimization design method for the machine tool's structural parts based on computer-aided engineering

Shihao Liu

Received: 29 September 2014 / Accepted: 9 December 2014 / Published online: 28 December 2014

Abstract In order to improve the static and dynamic performance of the machine tool's structural parts and achieve lightweight design at the same time, a multi-objective optimization design method is proposed. The orthogonal experimental design method and response surface method are adapted to establish the optimization model, while a modified particle swarm optimization algorithm and grey relational analysis method are adapted to solve the model. The proposed method was used to conduct multi-objective optimization design for a gantry machine tool's slide-seat. Based on the computer-aided engineering analysis, the response surface optimization model was established. After verifying the accuracy of response surface optimization model, five groups of non-inferior solutions are obtained by using the particle swarm optimization algorithm. The optimal design scheme was selected from the non-inferior solution set through using the grey relational analysis method, which reduces slide-seat's mass and improves its static and dynamic performance considerably. After conducting static and dynamic experimental study on the slide-seats before and after multi-objective optimization design, the rationality and feasibility of the multi-objective optimization design method for the machine tool's structural parts were verified.

Keywords Machine tool · Structural parts · Multi-objective optimization design · Computer-aided engineering

1 Introduction

With the positive development of mainland China's aerospace engineering, shipbuilding industry, marine engineering equipment, automotive, and other manufacturing industries, the processing demand of large and complex parts increases greatly; hence, the CNC machine tool develops with a considerable speed. In order to meet the high precision and efficient development trends of modern CNC machine tool as well as achieving structural lightweight design, the machine tool should also have high dynamic performance. Therefore, the structural design of the CNC machine tool is a multi-objective optimization issue, which is intensively researched by many scholars and machine tool design experts [1]. For instance, Guo et al. [2] conducted optimization design for a machine tool bed by using unit structure method, which can reduce the simulation modeling work in computer-aided engineering (CAE) analysis. Shen et al. [3] proposed a multi-objective optimization method for forging machine tool based on genetic algorithm, which improved the design efficiency and effectiveness of the forging machine tool. Zhao et al. [4] made structure optimization design for stiffener plate of a gantry machine tool's cross-beam based on giant waterlily vein distribution and summarized the bionic design principles of the cross-beam's stiffener plate. Yang et al. [5] made structural dynamic optimization design for a machine tool bed by using the CAE technology based on sensitivity analysis. Dai et al. [6] developed a three-dimensional parametric optimization design platform to optimize the main structural parts of a horizontal lathe based on the CAE technology. Jiang et al. [7] used a multi-objective genetic algorithm to conduct optimization design for a machining center, which made the whole structure lighter under the precondition of ensuring the static and dynamic performance.

The above research results do not only promote the development of the machine tool's structural part optimization design method, but they also provide many useful references for this paper's study. In the view of the geometric complexity and optimization objectives' diversity of the machine tool's structural parts, a multi-objective optimization design method

S. Liu (✉)
College of Mechanical and Electrical Engineering, Hainan University, Haikou, Hainan 570228, China
e-mail: liushihao1102@126.com

was established in this paper. The orthogonal experiment method and response surface method were used to build the approximate model based on computer-aided engineering (CAE) analysis; the particle swarm optimization and grey relational analysis were taken as the solving method. Taking the slide-seat of a gantry machine tool as the research object, the structural optimization design was conducted and combined with the static and dynamic experiments, which showed that the proposed multi-objective optimization design method of the machine tool's structural parts was valid.

2 Machine tool structural parts' multi-objective optimization model

The mathematical model of multi-objective optimization design regularly contains objective functions, design variables, and constraint functions. The objective function is the functional relationship between optimization objective and design variables. The constraint function is the restrictive condition to solve the minimum of the objective function [8]. Based on the theoretical analysis mentioned above, the multi-objective optimization problem of the machine tool's structural parts design can be expressed as the following mathematical model.

$$\begin{cases} \min\ Y = F(X) = \{F_1(X), F_2(X), \cdots, F_m(X)\} \\ X \quad = \quad (x_1, x_2, \cdots, x_i, \cdots, x_n) \\ s.t. \quad \begin{cases} g_u(x) \le 0 (u = 1, 2, \cdots, k < n) \\ h_v(x) = 0 (v = 1, 2, \cdots, p < n) \end{cases} \\ x_{il} \le \quad x_i \le \quad x_{im} (i = 1, 2, \cdots, n) \end{cases} \tag{1}$$

In the above optimization mathematical model (1), x_i is the design variable and Y is the state variable. $F_k(x)(k = 1, 2,\ldots,m)$ is the objective function. $g_u(x) \le 0$ and $h_v(x)=0$ are inequality constraint functions and equality constraint functions, respectively. x_{il} and x_{im} are lower limit and upper limit of the design variable respectively. m, k, p, and n are the number of the objective functions, inequality constraint functions, the equality constraint functions, and design variables, respectively.

2.1 Optimization objective

The machine tool's structural part optimization design is to meet certain processing accuracy requirements, which should allow the static and dynamic performance to achieve the optimal design goals. In this paper, the machine tool's structural part optimization objective functions are as follows.

2.1.1 Lightweight design

In the working process of a machine tool, the machine tool's structural parts are likely to be needed to achieve the feed motion driven by screw-nut mechanism. In order to ensure accurate positioning of the feed motion and save materials in machine tool manufacturing, the mass of machine tool's structural parts should be as light as possible.

$$\text{Min } M(X) \quad = \rho V(x_1, x_2, \ldots, x_m) \tag{2}$$

2.1.2 High anti-vibration performances

As an important part of the machine tool, the structural parts' anti-vibration performance directly affects the dynamic performance of the whole machine. Therefore, the machine tool's structural parts need strong anti-vibration performance, whose first few orders natural frequencies (f_1,f_2,$\cdots$,f_n) should be as high as possible.

$$\begin{aligned} &\text{Max } f(f_1, f_2, \cdots, f_n) \\ &\quad = \max((\alpha_1 f_1 + \alpha_2 f_2 + \cdots + \alpha_n f_n)) \end{aligned} \tag{3}$$

2.1.3 Optimal static performances

In order to improve the anti-cutting ability of the machine tool, excellent static performance of structural parts is essential. It means that the maximum deformation and the maximum stress of the machine tool's structural parts under working condition can be considered as the optimization objectives. The principle of the optimization design is to minimize the maximum deformation and the maximum stress.

$$F(X) \quad = \text{Min}(\sigma_{max}, \delta_{max}) \tag{4}$$

2.1.4 Optimal comprehensive performances

In the design process of the machine tool's structural parts, the machine tool's structural parts with optimal comprehensive performance should be obtained. Therefore, the objective functions are some of the above, which belongs to a multi-objective optimization design issue. The objective function can be described as follows.

$$\text{Min } F(X) = [f_1(X) \;\;, f_2(X), \ldots, f_{\mathrm{m}}(X)] \tag{5}$$

2.2 Constraints

The constraint is the technical conditions that the design scheme should meet. For the various functional machine tools, the constraints are also different. For a multi-objective optimization design issue, the objective function of a design problem may be a constraint of another design. The common constraints are as follows.

$$\begin{cases} \text{Strength constraint :} & \sigma_{\max} - [\sigma] \leq 0 \\ \text{Stiffness constraint :} & \delta_{\max} - [\delta] \leq 0 \\ \text{Stability constraint :} & \sigma_{cr} - \sigma_p \leq 0 \end{cases} \tag{6}$$

2.3 Design variables

During the multi-objective optimization design process of the machine tool's structural parts, the design variables are selected from the geometric dimensions (length L, width W, height H) and the thickness x_1, x_2,…, x_n of the stiffener plates. According to the selected design variables, other design variables can be described as these selected variables.

3 Solving method for multi-objective optimization of machine tool's structural parts

3.1 Response surface modeling techniques based on orthogonal experimental design

The machine tool's structural parts are generally very complicated and suffer a lot of highly constraints usually; therefore, the objective functions and constraints of multi-objective

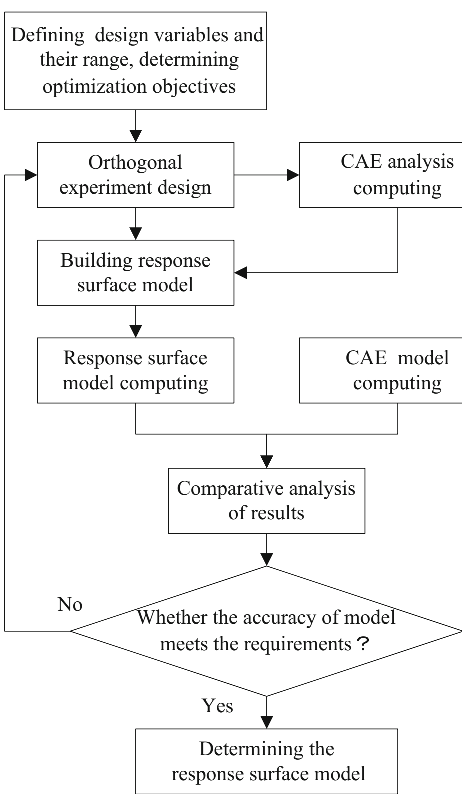

Fig. 1 Response surface modeling process

optimization mathematical model (1) are compound, implicit, and nonlinear functions related to design variables, which are difficult to build precisely. In order to solve the above problem, the response surface method is introduced to build multi-objective optimization mathematical model of the machine tool's structural parts by using CAE technology.

The response surface method is an approximate mathematical modeling approach, which has been introduced to conduct structural optimization design of mechanical engineering in recent years. The principle of response surface method is to obtain the response surface model of objective function about design variables via conducting experimental design on selected points and predict the value of non-experimented points [9, 10]. The theory of response surface method is illustrated below.

Assuming that the function relationship between response value $Y(X)$ and variable X is Eq. (7).

$$Y(X) = F(X) + \varepsilon = \sum_{i=0}^{L} a_i \varphi_i(X) + \varepsilon \tag{7}$$

$F(X)$ is an approximate function between optimization objective and design variables, which is response surface model. ε represents comprehensive errors that includes modeling errors, random errors, and others. L is the number of basic functions. The basic function ϕ_i(X) is polynomial function related to design variables XE_n. The second-order polynomial response surface model (as shown in Eq. (8)) with high calculating accuracy and solving efficiency is widely used to build the multi-objective optimization model of mechanical structure [11]. Hence, this model is adopted to optimize the machine tool's structural parts in this paper.

$$F(X) = a_0 + \sum_{i=1}^{n} a_i x_i + \sum_{i=1}^{n} a_{ii} x_i^2 + \sum_{i<j}^{n} a_{ij} x_i x_j \tag{8}$$

After obtaining the response vector F=(F (X_1), F (X_2),…., F (X_Q)) of Q design points ($Q \geq L$), the coefficient vector A=(a_0, a_1,…, a_L)^T of Eq. (8) can be solved via the least-square method. The least-square solving method can be described as in Eq. (9).

$$\begin{cases} E(\varepsilon) = \sum_{j=1}^{Q} \varepsilon^2 = \sum_{j=1}^{Q} \left\{ \left[Y(X) - \sum_{i=0}^{L} a_i \phi_i(X) \right]^2 \right\} \\ \frac{\partial E(\varepsilon)}{\partial a_i} \Big|_{a_i} = -2X^T Y + 2X^T X A = 0 \end{cases} \tag{9}$$

Then the vector A can be obtained from the Eq. (10).

$$A = \left(X^{\mathrm{T}} X\right)^{-1} X^{\mathrm{T}} Y \tag{10}$$

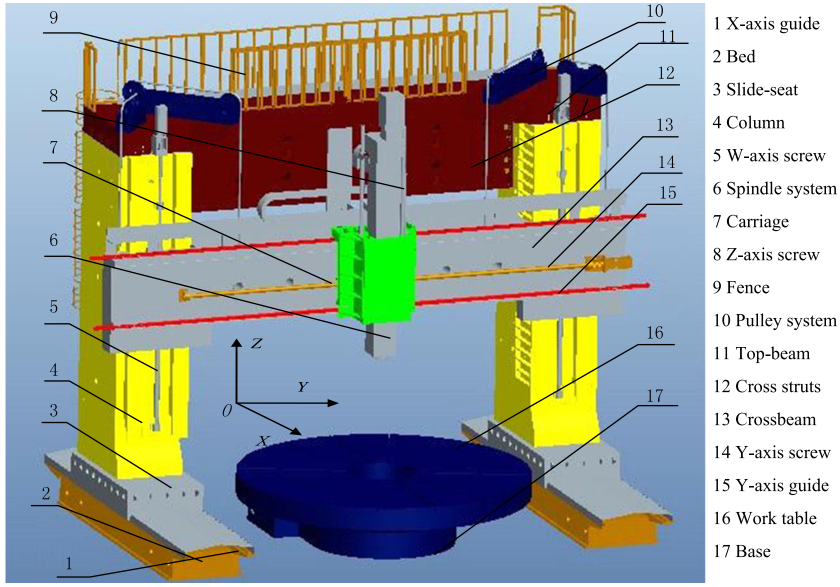

Fig. 2 3-D model of gantry machine tool

In Eq. (10), X is the basic function matrix, whose expression is illustrated with Eq. (11).

$$X = \begin{bmatrix} \phi_1(X_1) & \phi_2(X_1) & \cdots & \phi_L(X_1) \\ \phi_1(X_2) & \phi_2(X_2) & \cdots & \phi_L(X_2) \\ \vdots & \vdots & \ddots & \vdots \\ \phi_1(X_Q) & \phi_2(X_Q) & \cdots & \phi_L(X_Q) \end{bmatrix} \tag{11}$$

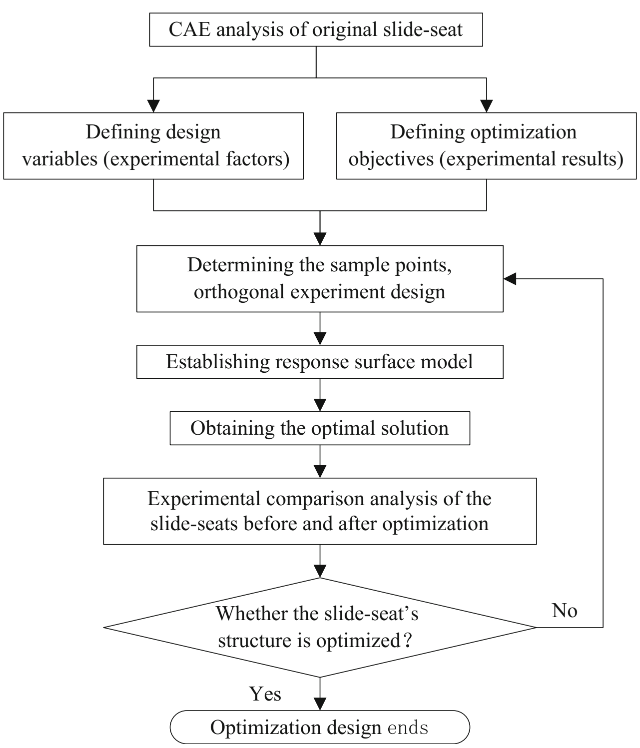

Fig. 3 Optimization design process

During building the response surface model, unsuitably selected testing points may reduce the accuracy of the response surface model, even make that the response surface model is unable to be obtained, while the experimental design theory can solve the above problem. The orthogonal experiment design is an experimental design method for multi-factors and multi-levels problems, which can utilize a few testing points to describe more information and define the number of orthogonal experiment's levels to satisfy the design requirements. Therefore, the orthogonal experimental design method is used to build response surface model in this paper. The accuracy of response surface model is ensured by comparing a number of response surface model's calculated values with the corresponding CAE model's calculated values. The implementation route of response surface modeling process is shown in Fig. 1.

3.2 Integration solving method of improved particle swarm algorithm and grey relational analysis

The solving process of multi-objective optimization problem of machine tool's structural parts consists of two steps: (1) solving the non-inferior solution set of multi-objective optimization function, (2) selecting an optimal solution from the non-inferior solution set to satisfy the design requirements.

In the view of optimization design theory, there are many non-inferior solutions after solving multi-objective optimization function. For the multi-objective optimization design

Table 1 Slide-seat's material parameters

Material	Density (kg/m^3)	Elastic modulus (GPa)	Poisson ratio
HT300	7800	180	0.3

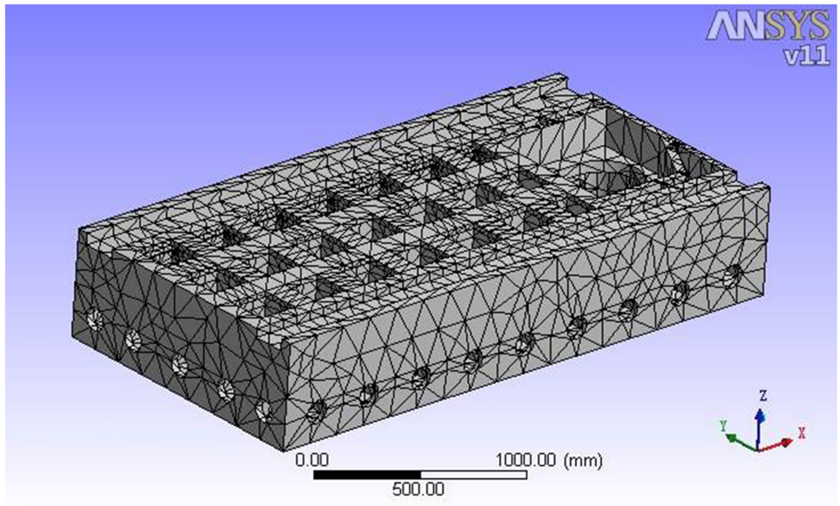

Fig. 4 CAE model of the original slide-seat

problem of the machine tool's structural parts, all of its non-inferior solutions constitute the non-inferior solution set or pareto optimal solution set. An optimization algorithm should be introduced to solve the pareto optimal set of the machine tool's structural parts multi-objective optimization.

Among the current optimization algorithms, particle swarm optimization (PSO) proposed by Dr Kennedy and Eberhart in 1995 is a global optimization algorithm based on swarm intelligence, which can find global optimal solution with high probability [12]. In recent years, the algorithm capacity of PSO has been enhanced by improving the control parameters, which has been successfully applied in many optimization solutions of mechanical engineering [13]. Therefore, in order to solve the multi-objective optimization design problem of the machine tool's structural parts, an improved multi-objective particle swarm optimization algorithm (DSMOPSO) based on crowding distance sorting proposed in literature [14] was adopted in this paper.

In order to select the optimal one from the non-inferior solution set, the machine tool design experts mainly judge with the subjective experience for lacking of a scientific optimum seeking method, which has certain degree of blindness and randomness. Usually, the fuzzy comprehensive evaluation method was adopted to solve this kind of multi-index and multi-scheme decision-making problem. However, the fuzzy evaluation matrix only considers each factor's contribution to optimal membership degree individually and can't reflect the influence of the each factor's coupling effect on optimal membership degree. The multi-index and multi-scheme decision-making problem contains both qualitative and quantitative information, so it can be regarded as a kind of grey information system. The grey relational analysis method proposed by Deng of Huazhong University of Science and Technology of China is an multi-objective optimum seeking method [15, 16], which is very suitable for addressing the above multi-objective optimization design problem. Therefore, the grey relational analysis method is adopted to select the optimal solution from the non-inferior solution set in this paper.

Assuming that there are n schemes in the non-inferior solution set of the multi-objective optimization issue of the machine tool's structural parts and each scheme has m indexes, the m indexes value can be expressed as vector x_i.

$$x_i = \left(x_{i,1}, x_{i,2}, \cdots, x_{i,m}\right) \tag{12}$$

Then, m indexes of n schemes in the non-inferior solution set can be expressed as the following matrix.

$$X = \begin{bmatrix} x_{1,1} & x_{1,2} & \cdots & x_{1,m} \\ x_{2,1} & x_{2,2} & \cdots & x_{2,m} \\ \vdots & \vdots & \ddots & \vdots \\ x_{n,1} & x_{n,2} & \cdots & x_{n,m} \end{bmatrix} \tag{13}$$

In order to conduct grey relational analysis conveniently, non-dimensional normalized treatment [17] is conducted on

Table 2 CAE analysis results of slide-seat

Static performance		Natural frequency/Hz			
Maximum deformation/mm	Maximum stress/MPa	The first order	The second order	The third order	The fourth order
0.0462	16.98	67.43	122.03	142.16	207.92

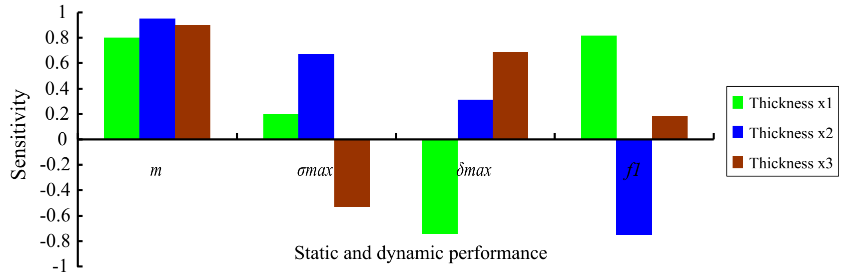

Fig. 5 The sensitivity analysis results

all evaluation index values of the non-inferior solution set. The treatment method is as follows.

1. For the bigger the better evaluation index

$$r_{i,j}=\frac{x_{i,j}-\min\left(x_{i,1},x_{i,2},\cdots,x_{i,m}\right)}{\max\left(x_{i,1},x_{i,2},\cdots,x_{i,m}\right)-\min\left(x_{i,m},x_{i,2},\cdots,x_{i,m}\right)} \tag{14}$$

2. For the smaller the better evaluation index.

$$r_{i,j}=\frac{-x_{i,j}+\max\left(x_{i,1},x_{i,2},\cdots,x_{i,m}\right)}{\max\left(x_{i,1},x_{i,2},\cdots,x_{i,m}\right)-\min\left(x_{i,1},x_{i,2},\cdots,x_{i,m}\right)} \tag{15}$$

Among them, j=1,2,⋯,m;k=1,2,⋯,n

After the normalized treatment, matrix (3) is as follows.

$$R=\begin{bmatrix} r_{1,1} & r_{1,2} & \cdots & r_{1,m} \\ r_{2,1} & r_{2,2} & \cdots & r_{2,m} \\ \vdots & \vdots & \ddots & \vdots \\ r_{n,1} & r_{n,2} & \cdots & r_{n,m} \end{bmatrix} \tag{16}$$

Because the n non-inferior solutions of the machine tool's structural parts has relativity of comparison, an ideal reference sequence is selected firstly, which is denoted as follows.

$$S^0=\left[s_1^0,s_2^0,\cdots,s_m^0\right] \tag{17}$$

In Eq. (17), s_j^0=max($r_{1,j}$,$r_{2,j}$,⋯,$r_{n,j}$), j=1,2,⋯,m, namely, each evaluation index of S^0 is the maximum value of corresponding evaluation indexes. S^0 is the ideal design scheme or reference sequence, while n schemes are comparison sequence. The close degree between reference sequence and comparison sequence is usually measured through the grey relational coefficient [15]. $\xi_{i,j}$ is the grey relational coefficient that the ith comparison sequence relatives to the jth index of reference sequence (i=1,2, …, n) . $\xi_{i,j}$ can be obtained from Eq. (18).

$$\xi_{i,j}=\frac{\min_i\min_j\left|s_j^0-r_{i,j}\right|+\rho\max_i\max_j\left|s_j^0-r_{i,j}\right|}{\left|s_j^0-r_{i,j}\right|+\rho\max_i\max_j\left|s_j^0-r_{i,j}\right|},\quad i=1,2,\cdots,n,\quad j=1,2,\cdots,m \tag{18}$$

In Eq. (18), $\rho \in [0, 1]$, thus, the grey relational coefficient matrix of non-inferior solution set of machine tool's structural parts multi-objective optimization design is Ξ.

$$\Xi=\begin{bmatrix} \xi_{1,1} & \xi_{1,2} & \cdots & \xi_{1,m} \\ \xi_{2,1} & \xi_{2,2} & \cdots & \xi_{2,m} \\ \vdots & \vdots & \ddots & \vdots \\ \xi_{n,1} & \xi_{n,2} & \cdots & \xi_{n,m} \end{bmatrix} \tag{19}$$

The η_{0i} is the grey relational degree that ith non-inferior

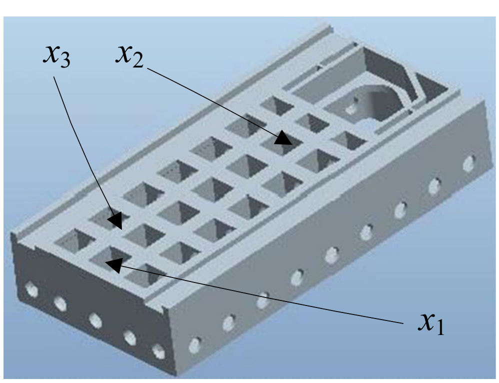

Fig. 6 Design variables of the slide-seat

Table 3 Factors and levels of orthogonal experimental design

Levels	Factors		
	x_1/mm	x_2/mm	x_3/mm
1	22	28	18
2	24	30	20
3	26	32	22
4	28	34	24

Table 4 Orthogonal experimental results of slide-seat

Number	Experimental factors			Experimental results			
	$x_1$mm	x_2/mm	x_3/mm	m/kg	σ_{max}/MPa	δ_{max}/mm	f_1/Hz
1	22	28	18	4276.42	25.43	0.0753	56.72
2	22	30	20	4477.48	23.19	0.0712	58.95
3	22	32	22	5033.22	16.14	0.0425	69.27
4	22	34	24	5067.08	15.37	0.0413	72.46
5	24	28	20	4462.74	22.56	0.0657	59.42
6	24	30	22	4838.46	16.21	0.0431	68.56
7	24	32	24	5143.42	14.39	0.0393	79.54
8	24	34	18	4704.94	17.32	0.0441	74.57
9	26	28	22	4576.38	22.48	0.0672	72.31
10	26	30	24	5077.42	13.21	0.0312	81.52
11	26	32	18	4681.78	18.34	0.0523	61.95
12	26	34	20	4974.68	17.25	0.0457	69.64
13	28	28	24	4562.98	23.71	0.0634	59.25
14	28	30	18	4638.74	22.58	0.0568	55.86
15	28	32	20	4943.68	16.07	0.0436	75.68
16	28	34	22 x_1	5279.42	12.85	0.0298	86.95

solution relatives to the ideal solution, which is expressed as follows.

$$\eta_{0i} = \frac{1}{m}\sum_{j=1}^{m}\xi_{i,j} i = 1, 2, \cdots, n, \quad j = 1, 2, \cdots, m \tag{20}$$

It can be acquired that the grey relational vector of n groups of non- inferior solutions is as follows.

$$R = (\eta_{01}, \eta_{02}, \cdots, \eta_{0n})^T \tag{21}$$

According to the grey relational degree vector R, the optimal design scheme of machine tool's structural parts optimization can be determined by comparing the $\eta_{0,1}, \eta_{0,2}, \cdots, \eta_{0,n}$.

Table 5 Different values of design variables

Group number	x_1/mm	x_2/mm	x_3/mm
Number 1 group	22	29	18
Number 2 group	23	30	19
Number 3 group	25	29	20
Number 4 group	26	31	21

4 Example application and experimental validation

The gantry machine tool studied in this paper is shown in Fig. 2, whose machining range is enough to be used for efficient processing of large and complex parts. The gantry machine tool was made by Wuxi Qiaolian CNC Machine Tool Co., Ltd, of China, and its power capacity is 37 Kw; spindle speed is 10~1500 rpm. The feed velocity of the gantry machine tool is as follow: 0~4 m/min in X-axis, 0~6 m/min in Y-axis, and 0~4 m/min in Z axis. Figure 2 shows that the slide-seat (part 3) plays a role in supporting the gantry frame structure, and it should achieve the X-axis feed motion on the bed, so the slide-seat must have good static and dynamic performance. In order to improve static and dynamic performance of the slide-seat, the multi-objective optimization design was conducted in according to the technology roadmap shown in Fig. 3.

4.1 CAE analysis of the original machine tool slide-seat

Machine tool slide-seat's material is the HT300, whose attribute parameters are shown in Table 1. The mass of original slide-seat is 4846.8 kg. The CAE model of the original slide-seat is shown in Fig. 4, which has 40,505 nodes and 21,428 elements. The unit type of slide-seat's finite element model is Solid45. The connection between slide-seat and screw-nut mechanism on bed was fixed constraints, and frictionless constraint was imposed on the contact surface between slide-seat and guide on bed to restrict the tangential displacement.

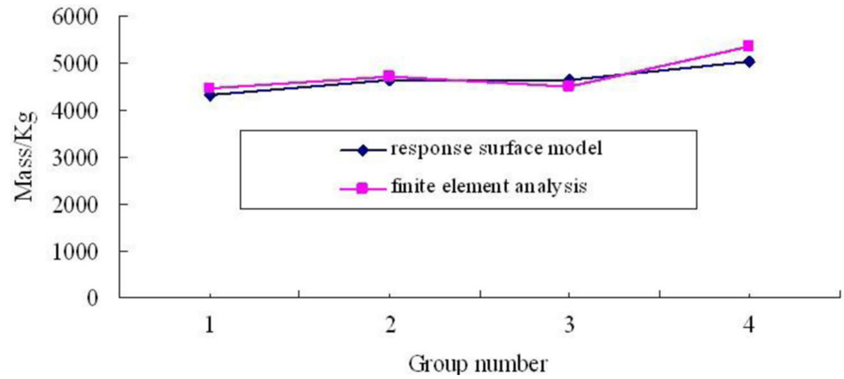

Fig. 7 Mass contrast

The loads imposed on the slide-seat are as follows: 3142 N in *X*-axis, 4257 N in *Y*-axis, and 28765 N in *Z*-axis. After completing the settings above, the structural and modal CAE analysis on the slide-seat were conducted through simulating the actual loading conditions, then the static and dynamic performance parameters obtained are shown in Table 2.

4.2 Machine tool slide-seat's multi-objective optimization modeling

In order to ensure the lightweight structure of the machine tool and improve the static and dynamic performance, the mass m, the maximum stress $\sigma_{\max}$, the maximum deformation $\delta_{\max}$, and the first order natural frequency f_1 of the slide-seat are taken as the optimization objective functions. The optimization design requirements of the above objective functions are as follows: the mass m, the maximum stress σ_{max}, and the maximum deformation δ_{max} should be as small as possible, whereas the first order natural frequency f_1 should be as high as possible. Since the slide-seat structure is very complex, the dynamic sensitivity analysis [18] was conducted and the analysis results are shown in Fig. 5. From Fig. 5, we can know that the thickness x_1 of the stiffener plate in *X*-axis direction has great influence on the maximum deformation and the first-order natural frequency, the thickness x_2 of the stiffener plate in *Y*-axis direction has great influence on the maximum stress and the first order natural frequency, and the influence of wall thickness x_3 has great influence on the maximum stress and the maximum deformation. Of course, the three thickness variables directly affect the mass of slide-seat. According to the dynamic sensitivity analysis results, x_1, x_2, and x_3 are selected as the design variables, which are shown in Fig. 6. The initial values of the design variables are x_1=25 mm, x_2= 30 mm, and x_3=20 mm. To meet the design requirements, each design variable ranges from 80 to 120 % of its initial value. In order to ensure the structural strength condition, the maximum stress of the slide-seat after multi-objective optimization design should be smaller than the material's allowable stress that is 50 MPa. Therefore, the mathematical model of the slide-seat's multi-objective optimization design is shown in formula (22).

$$\begin{cases} F(x_1,x_2,x_3) = \min(m,\sigma_{\max},\delta_{\max},-f_1) \\ m = F_m(x_1,x_2,x_3) \\ \sigma = F_\sigma(x_1,x_2,x_3) \\ \delta = F_\delta(x_1,x_2,x_3) \\ f_1 = F_f(x_1,x_2,x_3) \\ s.t \begin{cases} \sigma(x_1,x_2,x_3)\leq[\sigma] = 50\text{MPa} \\ 20\text{mm}\leq x_1\leq 30\text{mm} \\ 24\text{mm}\leq x_2\leq 36\text{mm} \\ 16\text{mm}\leq x_3\leq 24\text{mm} \end{cases} \end{cases} \tag{22}$$

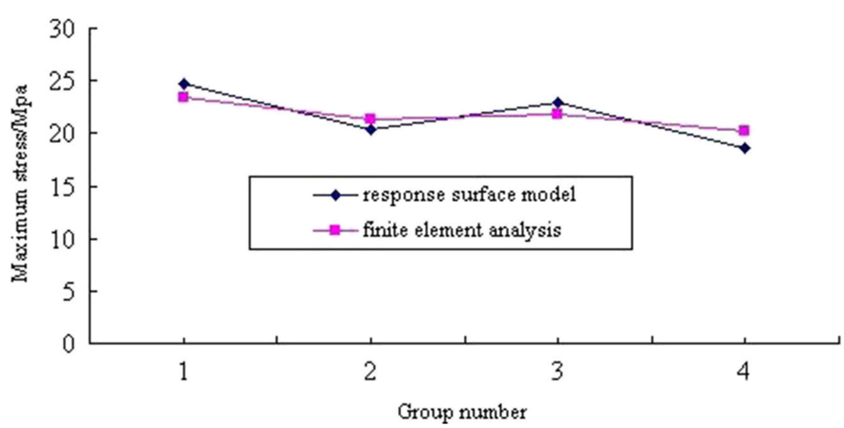

Fig. 8 The maximum stress contrast

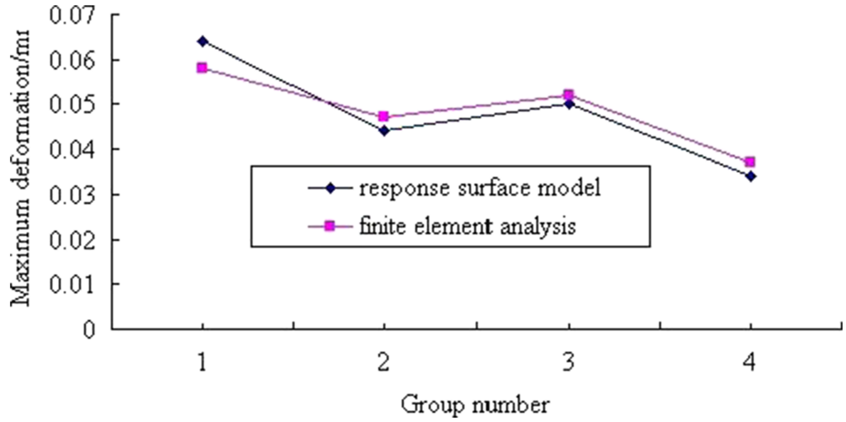

Fig. 9 The maximum deformation contrast

The design variables of machine tool slide-seat are a series of variable parameters within the allowable range. In order to obtain the optimal combination of design parameters, it will certainly conduct comparative analysis among a lot of design schemes. In order to reduce the CAE analysis times, the orthogonal experimental method was introduced to build the response surface approximation model of machine tool slide-seat's optimization design. The three design variables of slide-seat's multi-objective optimization design were taken as the orthogonal experiment's factors, and orthogonal table with four levels and three factors (shown in Table 3) was arranged in according to the permitted range of the variables. Then, $L_{16}(4^3)=16$ times CAE analysis were conducted. After completing all CAE analysis, the values of the design parameters (experimental factors) and the optimization objective functions (experimental results) are shown in Table 4.

4.3 Response surface optimization of machine tool slide-seat

4.3.1 Building response surface optimization model

After processing the data of Table 4 in MATLAB in accordance with Eq. (9) to (11), the coefficient vectors of $F_m(x_1,x_2,x_3)$, $F_\sigma(x_1,x_2,x_3)$, $F_\sigma(x_1,x_2,x_3)$ and $F_f(x_1,x_2,x_3)$ obtained are A_m=(−2416, 242.2, 567.2, 301.2, −4.284, −11.396, −0.9752, 14.978, 7.796, −4.114), A_σ =(167.8,2.726, −4.189, −5.004, 0.1274, 0.1633, −0.1447, −0.3918, 0.1887, 0.2106), A_δ=(0.5772, 0.004644, −0.02267, −0.002279, 0.0003536, 0.0005906, −0.0005737, −0.0009616,0.0004486, 0.0004909) and A_f=(200.2, 3.84, −9.643, 4.332, −0.452, −0.02318, 0.0567, 0.7556, −0.03848, 0.07395). Therefore, the machine tool slide-seat's multi-objective optimization response surface models are shown as Eq. (23), (24), (25) and (26).

$$\begin{aligned} F_m(x_1,x_2,x_3) &= -2416 + 242.2\,x_1 + 567.2\,x_2 + 301.2\,x_3 \\ &\quad -4.284\,x_1^2 - 11.396\,x_2^2 - 0.9752\,x_3^2 \\ &\quad + 14.978\,x_1x_2 + 7.796\,x_2x_3 - 4.114\,x_3x_1 \end{aligned} \tag{23}$$

$$\begin{aligned} F_\sigma(x_1,x_2,x_3) = {} & 167.8 \\ & + 2.726\,x_1 - 4.189\,x_2 - 5.004\,x_3 \\ & + 0.1274\,x_1^2 \\ & + 0.1633\,x_2^2 - 0.1447\,x_3^2 - 0.3918\,x_1x_2 \\ & + 0.1887\,x_2x_3 + 0.2106\,x_3x_1 \end{aligned} \tag{24}$$

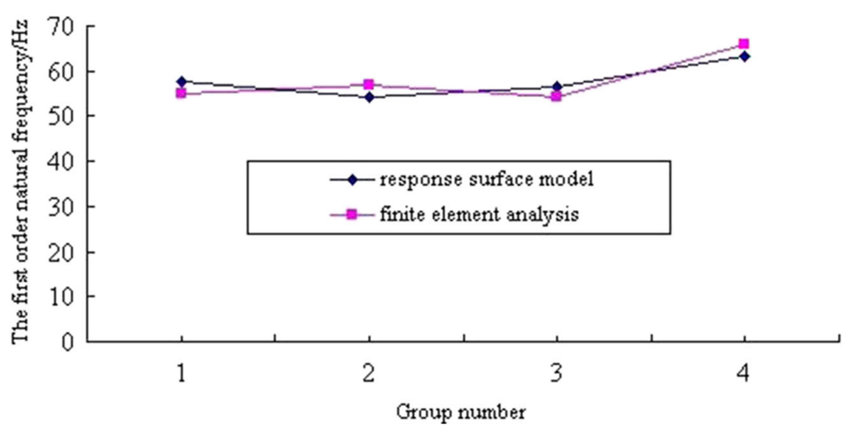

Fig. 10 The first natural frequency contrast

Table 6 Non-inferior solution set

Number	Design variables			Optimization objectives			
	$x_1$mm	x_2/mm	x_3/mm	m/kg	σ_{max}/MPa	δ_{max}/mm	f_1/Hz
A	26.425	30.683	21.359	4590.2	14.92	0.0398	73.58
B	24.518	29.154	20.236	4544.6	15.23	0.0476	74.47
C	23.341	28.563	19.148	4415.0	15.67	0.0423	75.62
D	21.373	27.452	19.642	4375.8	16.35	0.0542	70.41
E	20.587	26.543	18.421	4383.2	16.16	0.0413	72.86

$$
\begin{aligned}
F_\delta(x_1,x_2,x_3) = {} & 0.5772 + 0.004644\ x_1 - 0.02267\, x_2 - 0.002279\ x_3 \\
& + 0.0003536\ x_1^2\ + 0.0005906\ x_2^2 - 0.0005737\ x_3^2 \\
& - 0.0009616\ x_1x_2\ + 0.0004486\ x_2x_3 \\
& + 0.0004909\ x_3x_1
\end{aligned} \tag{25}
$$

$$
\begin{aligned}
F_f(x_1,x_2,x_3) = {} & 200.2 + 3.84\ x_1\ - 9.643\, x_2 \\
& + 4.332\ x_3\ - 0.452\ x_1^2\ - 0.02318\ x_2^2 \\
& + 0.0567\ x_3^2 \\
& + 0.7556\ x_1x_2\ - 0.03848\ x_2x_3 \\
& + 0.07395\ x_3x_1
\end{aligned} \tag{26}
$$

4.3.2 Verifying the accuracy of response surface model

Taking any four groups of non-interpolation points shown in Table 5, after comparing the calculated values of response surface model with corresponding CAE analysis calculated values, the comparative results obtained are presented from Fig. 7 to Fig. 10. Figures 7, 8, 9, and 10 show that the calculated results between response surface model and CAE model are very close and all the errors are about 5 %. Therefore, the accuracy of slide-seat's response surface models built in this paper is reliable, and response surface models can be used to solve the slide-seat's multi-objective optimization design problem.

Table 7 Objective functions contrast

Comparison of indexes	Mass/kg	Maximum stress/Mpa	Maximum deformation/mm	The first natural frequency/Hz
Initial scheme	4846.8	16.98	0.0462	67.43
Optimization scheme	4415.2	15.67	0.0423	75.62
Rate of change (%)	−8.91	−7.71	−8.44	+12.15

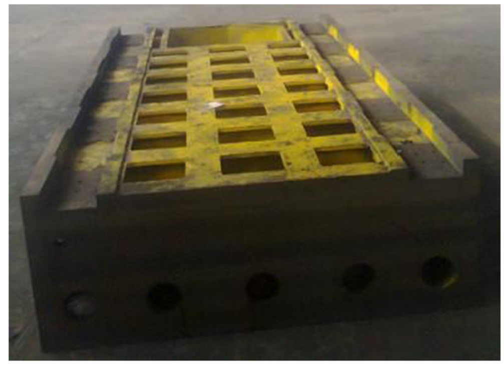

Fig. 11 Physical model of machine tool slide-seat

4.4 Results analysis of slide-seat's multi-objective optimization

The machine tool slide-seat's multi-objective optimization response surface models were solved via DSMOPSO algorithm programming with the help from MATLAB software, and then five groups of non-inferior solutions obtained are shown in Table 6.

After processing the data of Table 6 according to Eq. (13)–(21), the grey relational degree of the five groups of non-inferior solutions obtained is R=(0.7235, 0.5648, 0.7691, 0.4998, 0.6558)^T. Therefore, the comprehensive evaluation order of the slide-seat's optimization design schemes is C>A>E>B>D, which means that the design scheme C is the best option. The slide-seat's objective functions values before and after optimization design are shown in Table 7, and the results show that 8.91 % of the mass of the slide-seat is reduced, the maximum stress decreases by 7.71 %, the maximum deformation decreases 8.44 %, and the first order natural frequency increases 12.15 %.

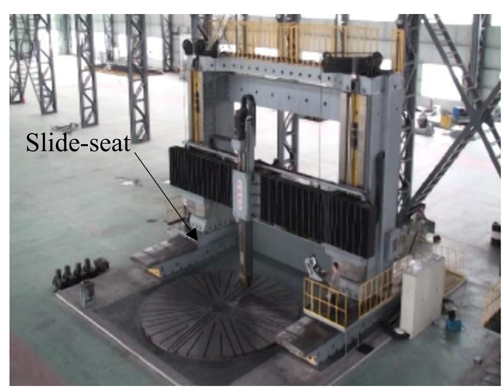

Fig. 12 Physical model of gantry machine tool

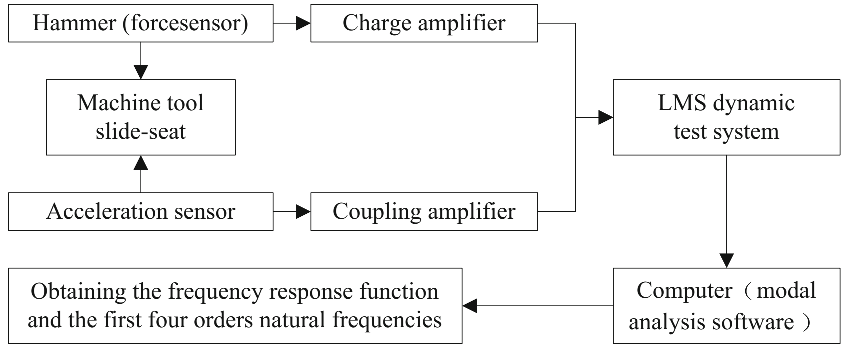

Fig. 13 Principle of dynamic experiment

The slide-seat manufactured according to the optimization design scheme C is shown in Fig. 11. Figure 12 shows the gantry machine tool's physical model after the slide-seat's optimization design. The slide-seat assembles well enough on the whole machine that the machining precision of the gantry machine tool is ensured after optimization design, which proves that the purpose of optimization design has been achieved.

4.5 Experimental verifying of slide-seat's optimization design

4.5.1 Experimental purposes

In order to verify the correctness of the multi-objective optimization design method for the machine tool's structural parts proposed in this paper, the static and dynamic experiments on the machine tool slide-seat before and after the optimization design were conducted in a closed laboratory with constant temperature.

4.5.2 Experimental principle

The purpose of the machine tool slide-seat's static experiment is to obtain the mass of the slide-seat, and the experimental equipment is weighbridge. The static experimental method and process are relatively simple; thus, no details are included within this paper, but only the experimental results are given. The purpose of the machine tool slide-seat's dynamic experiment is to obtain the first four orders natural frequencies, and the principle of dynamic experiment is shown in Fig. 13. After selecting the proper test points on slide-seat, the dynamic test system were installed properly in according to the principle model shown in Fig. 13, and then the excitation force signal and corresponding response signal of each point can be acquired. With the modal analysis software, the frequency response function of test points can be analyzed, and the slide-seat's natural frequencies can be identified by analyzing the frequency response function curve.

4.5.3 Experimental conditions and apparatus

The slide-seat's dynamic experimental equipment is shown in Fig. 14. During the dynamic experiment process, the ambient temperature was 25 °C. The experimental apparatus are as follows: the exciter (The top of exciter is force sensor, sensitivity 0.2216 mv/N), the acceleration sensor (sensitivity 99.1 mv/N in the X-axis direction, 99 mv/N in Y-axis direction, and 106.1 mv/N in Z-axis direction), the dynamic test system, and the computer. The exciter was used to excite the slide-seat. The force sensor was used to pick up the excitation signal and convert it into charge signal. The acceleration sensors were used to pick up the response signal and convert it into charge signal. The dynamic test system produced by the Belgium LMS company was used to acquire and process experimental data. The modal analysis software is the LMS Test Lab analysis system that matches the LMS dynamic test system. The slide-seat's dynamic experiments were carried out in a closed constant temperature laboratory of Wuxi Qiaolian

Fig. 14 Dynamic experimental equipment

Table 8 Parameters contrast

Comparison of indexes	Initial scheme	Optimization scheme	Rate of change (%)
Mass/Kg	4844.3	4414.6	−8.89
The first natural frequency/Hz	68.21	76.23	+11.17
The second natural frequency/Hz	121.98	131.02	+7.42
The third natural frequency/Hz	143.02	154.98	+8.32
The fourth natural frequency/Hz	207.86	229.31	+10.31

CNC Machine Tool Co., Ltd. The typical process for frequency measurements is as follows:

1. The dynamic test system was installed well according to the dynamic experiment principle (Fig. 13).
2. The excitation force was applied to the excitation point by exciter, and the acceleration sensor was fixed on test points to pick up the acceleration response signal.
3. After setting the related parameters in modal analysis software, the excitation force signal and acceleration response signal of the test points on slide-seat were collected.
4. The excitation force signal and acceleration response signal was input to the computer.
5. After conducting modal analysis in computer, the first four order natural frequencies of slide-seat were obtained.

4.5.4 Analysis of experimental results

After completing the static and dynamic experiments, the experimental results of static and dynamic performance parameters of the machine tool slide-seat are shown in Table 8. If the slide-seat's natural frequencies increase after optimization design, the correctness of the multi-objective optimization design method is verified. Table 8 shows that the slide-seat's mass is reduced and anti-vibration performance is improved further after optimization design, which proves that the multi-objective optimization design method for the machine tool's structural parts proposed in this paper is reasonable and feasible.

5 Conclusions

1. The novelty of this paper is that a multi-objective optimization design method for the machine tool's structural parts is proposed. The proposed method can cut the number of tests by using the orthogonal experimental method to build response surface model, and avoid the randomness by using grey relational analysis method to select the optimal solution from the non-inferior solution set. Therefore, it does not only provide a new approach for the machine tool's structural optimization design, but the proposal also has strong reference value for multi-objective optimization design of other mechanical parts.
2. Based on the CAE analysis, mathematical model of the slide-seat's multi-objective optimization design was established. The second-order response surface method based on orthogonal experimental design was used to build the optimization model for slide-seat, and particle swarm optimization algorithms and grey relational analysis method were used to obtain the optimal solution, which expands the applications of these mathematical methods and has important theoretical significance.
3. During the optimization design process of gantry machine tool's slide-seat, in order to solve the conflict between the static and dynamic performance and lightweight design, the multi-objective optimization design was conducted. After the optimization design, the mass was reduced, the static performance was improved, and the first natural frequency was increased. The feasibility and correctness of the proposed multi-objective optimization design method were verified by static and dynamic experiments.

Acknowledgments The work is supported by National Natural Science Foundation of China (Grant No.51405115) and the scientific research foundation of Hainan University (kyqd1431).

References

1. Li BT, Hong J, Liu ZF (2014) Stiffness design of machine tool structures by a biologically inspired topology optimization method. Int J Mach Tool Manuf 84:33–44
2. Guo L, Zhang H, Wang JS, Ye PQ (2011) Theoretical modeling and verifications of unit structure method. J Mech Eng 47(23):135–143
3. Shen Y, Jin Y, Chu B, Luo NW, Zhu CA (2012) A multi-objective optimization method for forging machine based on genetic algorithm. China Mech Eng 23(3):291–294
4. Zhao L, Chen WY, Ma JF (2008) Structural bionic optimization of stiffening ribs of a machine tool crossbeam based on giant waterlily vein distribution. High Tech Lett 18(8):806–810
5. Yang Y, Zhang WM, Li PZ (2011) Structure optimization design for NC machine bed based on dynamic sensitivity analysis. J Mach Des 29(9):49–52
6. Dai L, Guan ZQ, Shan JL, Niu CM, Zhang HW, Gu YX (2008) 3D parameterized shape optimization design for machine tool mechanism. J Mech Eng 44(5):152–159
7. Jiang H, Guan YS, Qiu ZC, Zhang XM, Chen Z, Xu G (2011) Dynamic and static multi-objective optimization of a vertical machining center based on response surface method. J Mech Eng 47(11):125–132
8. Sun GY, Li GY, Gong ZH (2009) Application in sheet metal forming optimization based on variable complexity model of metamodeling technique. J Mech Eng 45(9):201–209
9. Hambli R, Mkaddem A, Potiron A (2005) Application of response surface method for FEM bending analysis. Int J Veh Des 39(1–2):1–13
10. Ahmadi SY, Khalili K, Eftekhari SE, Kang BS (2014) Loading path optimization of a hydroformed part using multilevel

response surface method. Int J Adv Manuf Technol 70(5–8): 1523–1531

11. Kankar PK, Harsha SP, Kumar P, Sharma C (2009) Fault diagnosis of a rotor bearing system using response surface method. Eur J Mech - A/Solids 28(4):841–857
12. Zhu HH, Wang Y, Wang KS, Chen Y (2011) Particle swarm optimization (PSO) for the constrained portfolio optimization problem. Expert Syst Appl 38(8):10161–10169
13. Shen J, Han LC, Shen YB (2008) Optimization of airplane primary parameters based on particle swarm algorithm. Acta Aeronaut Et Astronaut Sin 29(6):1538–1541
14. Li ZK, Tan JR, Feng YX, Fang H (2008) Multi-objective particle swarm optimization algorithm based on crowding distance sorting and its application. Comput Integr Manuf Syst 14(7):1329–1333
15. Fan CK, Tsai HY, Lee YH (2008) The selection of life insurance sales representatives training program by using the AHP and GRA. J Grey Syst 20(2):149–160
16. Xiao YH, Liu YL, Yang H, Ren JB (2014) Optimization of processing parameters for double-ridged rectangular tube rotary draw bending based on grey relational analysis. Int J Adv Manuf Technol 70(9–12):2003–2011
17. Liu SH, Ye WH, Chen WF, Yang Q, Hu ZH (2010) Design plan optimum seeking of machine tool bed based on grey relational analysis. J Grey Syst 22(4):341–352
18. Abdessalem A, El-Hami A (2014) Global sensitivity analysis and multi-objective optimisation of loading path in tube hydroforming process based on metamodelling techniques. Int J Adv Manuf Technol 71(5–8):753–773